WORLD JOURNAL OF PHARMACEUTICAL RESEARCH
SJIF Impact Factor 8.084
Volume 9, Issue 4, 26-47. Research Article ISSN 2277– 7105

SYNTHESIS OF ORGANOTIN POLYETHERS FROM CHLORAMPHENICOL AND THEIR ABILITY TO INHIBIT A BROAD RANGE OF HUMAN CANCER CELL LINES INCLUDING PANCREATIC, BREAST, AND BRAIN CANCERS

Charles E. Carraher Jr.*[1], Zachary Rabinowitz[1], Michael R. Roner[2], Paul Slawek[1], Francesca Mosca[1], Jessica Frank[1] and Lindsey C. Miller[2]

[1]Florida Atlantic University, Department of Chemistry and Biochemistry, Boca Raton, FL 33431.

[2]University of Texas Arlington, Department of Biology, Arlington, TX 76010.

Article Received on
25 Jan. 2020,
Revised on 15 Feb. 2020,
Accepted on 06 March 2020
DOI: 10.20959/wjpr20204-17049

***Corresponding Author**
Charles E. Carraher Jr.
Florida Atlantic University, Department of Chemistry and Biochemistry, Boca Raton, FL 33431.

ABSTRACT

Organotin polymers were rapidly synthesized from the antibiotic chloramphenicol in moderate yield employing the interfacial polymerization process. Percentage yield increases as the size of the alkyl-tin moiety increases and the chain length decreases consistent with steric hindrance playing a role in product chain growth. Infrared spectroscopy showed the formation of Sn-O ester units. Matrix assisted laser desorption mass spectroscopy (MALDI) showed the formation of ion fragments consistent with the presence of tin-containing polyethers. The polymers showed good inhibition of all tested human cancer cell lines including pancreatic, breast, and brain cancers thus offer a new family of materials that exhibit the ability to inhibit a broad range of human cancers.

KEYWORDS: Metal-containing polymers, organotin containing polymers, chloramphenicol, brain cancer, breast cancer, pancreatic cancer, organotin polyesters, interfacial polymerization.

INTRODUCTION

The emphasis in this particular research is the synthesis of organotin-based polymers that may exhibit anticancer properties. Although organotin-based compounds have many

important applications and uses, they are of interest as medicinal agents due to several factors including their molecular geometry, availability of coordination positions at the tin atom, the occurrence of relatively stable ligand-Sn bonds, and low hydrolytic decomposition.[1] One of the main uses of organotin compounds is as biocides in industry and agriculture due to their high antifungal properties.[2] The ability for organotins to inhibit cancer has been known for over 70 years. This has been reviewed.[3]

We have been including into metal-containing polymers drugs that themselves offer biological activities hoping for the combination to enhance the ability of the resulting materials to inhibit cancer.[4-18] This paper describes one of these efforts.

Advantages of Polymeric Drugs. Due to unique properties of polymers, the use of polymeric drugs has several potential advantages over small, monomeric drugs. The following includes some of these advantages briefly described. First, a polymer should be excreted by the kidneys more slowly than small compounds, which decreases kidney damage and increases the bioavailability of the drug. Second, polymers are more limited with respect to their travel within the human body because of their size. By delivering the active polymeric drug to the specific target site, the mobility of the drug is limited. This allows for a reduction of negative side effects and an enhanced activity. Third, coupling of two drug components may allow synergetic effects to occur. Design of the components of the polymeric drug can allow the incorporation and subsequent activity of drugs that act differently but in a combined manner to eradicate disease, or one might act to entice a cancer cell to accept part of the polymer combination with the second part carrying either a therapeutic or toxic "sting". Fourth, in the treatment of many diseases, including cancer, multiple attachments to the DNA or to a specific protein might increase the drug's chances of being successful, and the capacity for such multiple attachments increases for polymer drugs. Fifth, cancer cells have rough cell surfaces that can "snag" polymers allowing a longer time for the drug to effectively inhibit the cancer cell. Lastly, most of the metal-containing condensation polymers exhibit poor stability in the presence of base, but good stability in the presence of acid. If the drugs are to be taken orally, this allows the drug to bypass degradation in the stomach, which is acidic, and to move further along the digestive canal where the basic surroundings encourage polymer degradation.[19]

Chloramphenicol. Chloramphenicol, Figure 1, is an antibiotic employed in the treatment of several bacterial infections including meningitis, conjunctivitis, cholera, and typhoid fever. It

was discovered in 1947 after being isolated from *Streptomyces venezuelae*, a species of soil-dwelling Gram-positive bacterium of the genus Streptomyces. In 1949, its chemical structure was determined and was the first antibiotic to be artificially made instead of extracted from a micro-organism. Chloramphenicol is highly lipid-soluble and remains relatively unbound to protein. It has a large apparent volume of distribution and thus, it penetrates all tissues of the body, including the brain. However, the distribution is not even. The highest concentrations of the drug are found in the liver and kidney, while the lowest are found in the brain and cerebrospinal fluid. In vitro, chloramphenicol exerts a bacteriostatic effect on a wide range of gram-negative and gram-positive bacteria, including Salmonella typhi and Hemophilus influenza. The mode of action is through interference or inhibition of protein synthesis in intact cells and in cell-free systems. Specifically, it prevents protein chain elongation by inhibiting the peptidyl transferase activity of the bacterial ribosome. It does so by binding to A2451 and A2452 residues in the 23S rRNA of the 50S ribosomal subunit.[20] Currently, its medical uses are limited due to adverse effects such as aplastic anemia, bone marrow suppression, gray baby syndrome, and hypersensitivity and neurotoxic reactions. For example, the World Health Organization (WHO) no longer recommends first-line only chloramphenicol to treat meningitis, however, recognizes it may be used with caution if there are no available alternatives.[21] Nevertheless, a 2017 systematic review found moderate evidence that using chloramphenicol eye drops in addition to an antibiotic injection will likely lower the risk of endophthalmitis, which is a complication of cataract surgery. It is sold under a number of names including chlornitromycin, chloromycetin, levomycetin and chlorocid. Overall, coupling of chloramphenicol with organotin was employed in the hopes of a synergetic effect to occur considering chloramphenicol's medicinal properties.

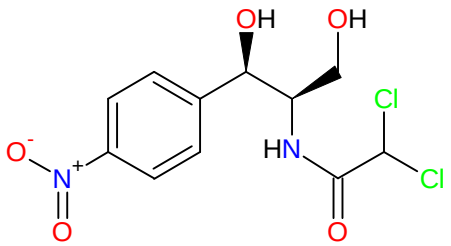

Figure 01: Structure of chloramphenicol.

EXPERIMENTAL

Chemicals and Materials: Diphenyltin dichloride (1135-99-5), dibutyl dichloride (683-18-1), and dimethyltin dichloride (753-73-1) were purchased from Aldrich Chemical Co.,

Milwaukee, WS. Diethyltin dichloride (866-55-7) was obtained from Peninsular Chemical Res., Gainesville, Fl. Dioctyltin dichloride (3542-36-7) was obtained from Ventron Alfa Inorganics, Beverly, Mass. Chloramphenicol (56-75-7) was obtained from Aldrich Chemical Co., Milwaukee, WS.

Synthesis: Reactions were carried out using the interfacial polycondensation technique. Briefly, an aqueous solution (30 mL) containing chloramphenicol (0.00300 mol) and sodium hydroxide (0.00600 mol) was transferred to a one-quart Kimax emulsifying jar fitted on top of a Waring Blender (model 1120; no load speed of about 18,000 rpm; reactions were carried out at about 25 ℃). Stirring was begun and a heptane solution (30 mL) containing the organotin dihalide (0.00300 mol) was rapidly added (about 3-4 seconds) through a hole in the jar lid using a powder funnel. The resulting solution was blended for 15 seconds. The precipitate was recovered using vacuum filtration and washed several times with deionized water and hexane to remove unreacted materials and unwanted by-products. The white solid was washed onto a glass Petri dish and allowed to dry at room temperature for one week in the fume hood. The product was weighted, and their yields recorded. Drying of products was confirmed by IR by the absence of bands characteristics of the solvents used- acetone, water, and heptane.

The polymer repeat unit is shown in Figure 2 where R' is simply the chain extension.

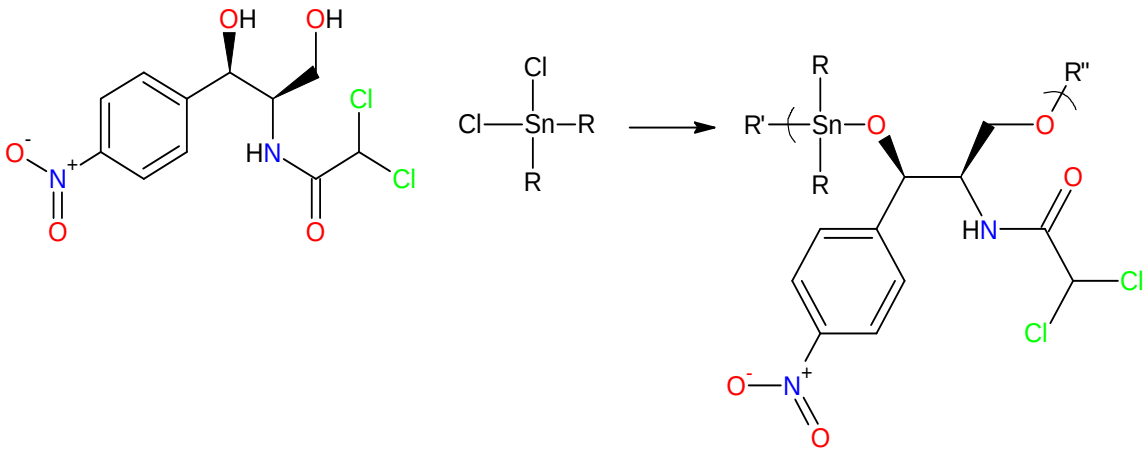

Figure 02: Structure of the repeat polymer unit.

Structural Characterization: Light scattering photometry was carried out in DMSO employing a Brice-Phoenix Universal Light Scattering Photometer Model 4000. Infrared spectra were obtained employing attenuated total reflectance infrared spectroscopy utilizing a

JASCO FT/IR-4100 fitted with an ATR Pro 450-s. High resolution electron impact positive ion matrix assisted laser desorption ionization time of flight, HR MALDI-TOF, mass spectrometry was carried out employing a Voyager-DE STR BioSpectrometer, Applied Biosystems, Foster City, CA. The standard settings were used with a linear mode of operation and an accelerating voltage of 25,000 volts; grid voltage 90% and an acquisition mass range of 500 to 100,000. Fifty to two hundred shots were typically taken for each spectrum. Results employing graphite are included in the present paper. Addition of graphite was accomplished by simply "drawing" on the matrix sample holder assembly using a number 2 pencil and placing the powered polymer sample on top of the graphite drawing.

Cell Testing: The toxicity of each test compound was evaluated against a battery of cancer cell lines. Following a 24 h incubation period, the test compounds were added at concentrations ranging from 0.0032 to 32,000 ng/mL and allowed to incubate at 37°C with 5% CO_2 for 72 h. Following incubation, Cell Titer-Blue reagent (Promega Corporation) was added (20 microL/well) and incubated for 2 h. Fluorescence was determined at 530/590 nm and converted to % cell viability versus control cells.

All cytotoxicity values are calculated against a base-line value for each line that was generated from "mock-treatment" of the normal and tumor cell lines with media supplemented with all diluents used to prepare the chemotherapeutic compounds. For example, if the compounds were dissolved in DMSO and serial dilutions prepared in Modified Eagle's Medium, MEM, to treat the cells, then the mock-treated cells were "treated" with the same serial dilutions of DMSO without added chemotherapeutic compound. This was done to ensure that any cytotoxicity observed was due to the activity of the compound and not the diluents. For the studies reported here, the mock-treatment never resulted in a loss of cell viability of more than one percent, demonstrating that the activity observed was not due to cytotoxicity of any of the diluents used, but was due to activity of the tested compounds. Once inhibition begun, the slope of the inhibition verses concentration was steep ending with total inhibition.

RESULTS AND DISCUSSION

Yield and Chain Length: The reactions occur rapidly, within 15 seconds, consistent with the rapidity of typical reactions between diols and the organotin acid chloride employing the interfacial polycondensation.[22,23] The product yield, molecular weight, and chain length of the synthesized polymeric materials appear in Table 1.

Table 01: Product yield, molecular weight and chain length (DP) as a function of organotin moiety for the reaction of organotin dihalides with the antibiotic chloramphenicol.

Organotin Moiety	% Yield	Mol. Wt. (Daltons)	DP
Me_2Sn	15	1.6×10^6	3800
Et_2Sn	36	1.1×10^6	2200
Bu_2Sn	43	2.8×10^5	500
Oc_2Sn	45	3.1×10^5	460
Ph_2Sn	53	2.1×10^6	390

The chain length or degree of polymerization (DP) varies from 3800 to 460. It decreases as the organotin alkyl group increases in bulk, which is consistent with steric hindrance playing a role in product chain growth. The percent yield increases as the organotin alkyl chain length increases. As the chain length increases, the organotin dihalide's solubility in the organic phase increases and in the aqueous phase, their solubility decreases. It is hypothesized that bulkier, less water soluble organotin dihalides are protected from premature hydrolysis, allowing for a more complete reaction. This result allows for the organotin acid chloride to have greater access to the aqueous phase with subsequent hydrolysis occurring to a lesser extent, consistent with the observed increased yield.

Infrared Spectroscopy: While infrared spectra were obtained for all of the products and monomers the emphasis here will be for only two of the representative products, those derived from dibutyltin and diphenyltin dichlorides. The IR spectra for chloramphenicol, dibutyltin dichloride and diphenyltin dichloride and their associated polymers appear in Figures 3-7 and assignments are given in Tables 2-5. Band assignments are given in wavenumber (cm^{-1}) and are based on previous literature.[24]

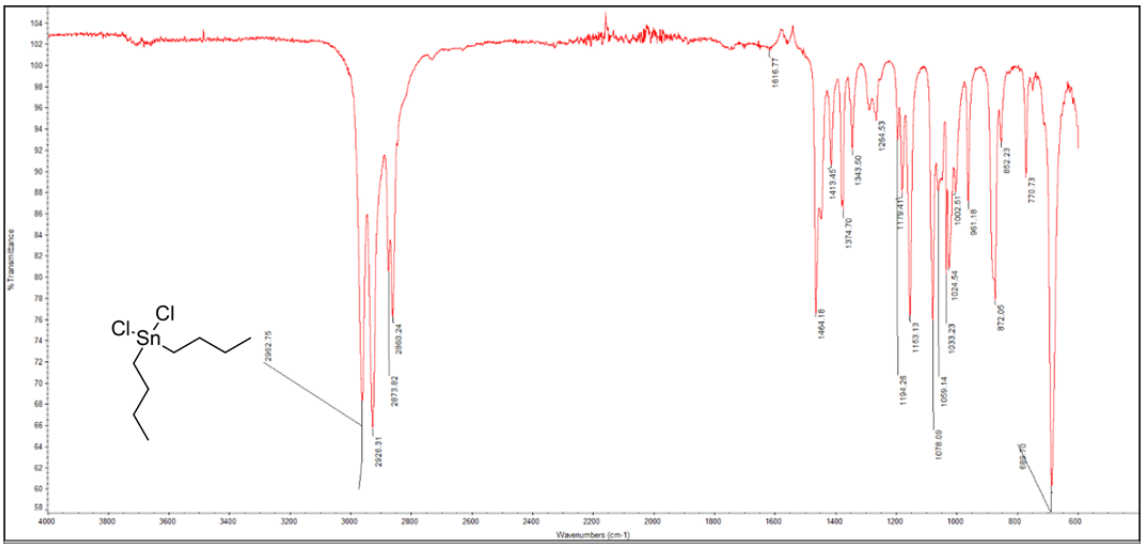

Figure 03: IR spectrum of Bu_2SnCl_2.

Table 02: Infrared Absorption Band Assignments for Bu_2SnCl_2.

Wavenumber (cm^{-1})	Assignment
2959	CH_3 Asymmetric Stretch
2927	CH_2 Asymmetric Stretch
2872	CH_3 Symmetric Stretch
2858	CH_2 Symmetric Stretch
1463	CH_3 Asymmetric Bending
1380	CH_3 Symmetric Bending
1178	C-C Stretch
1152	C-C Stretch
878	CH_3 Rocking
592	Sn-C Asymmetric Stretch
509	Sn-C Symmetric Stretch

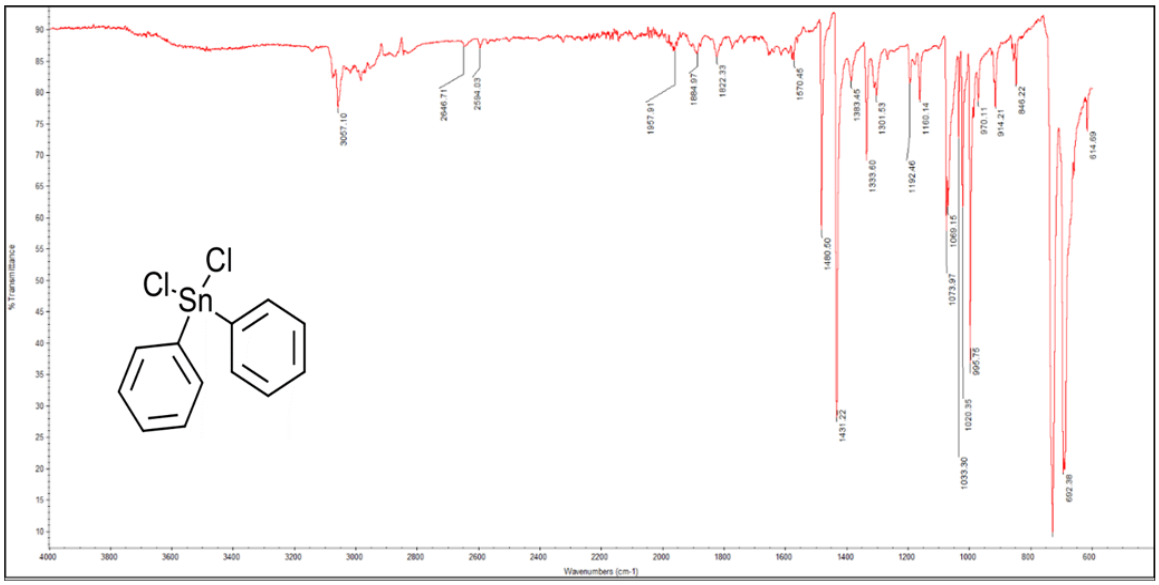

Figure 04: IR spectrum of Ph_2SnCl_2.

Table 03: Infrared Absorption Band Assignments for Ph_2SnCl_2.

Wavenumber (cm^{-1})	Assignment
3068	Aromatic C-H Stretch
3057	Aromatic C-H Stretch
1480	Sn-C_6H_5 Stretch
1431	C=C Stretch
1334	C=C Stretch
1074	Sn-C_6H_5 Stretch
996	Ring vibration
729	Symmetric Out-of-Plane Bending
692	Asymmetric Out-of-Plane Bending
442	Asymmetric Stretch Sn-C_6H_5

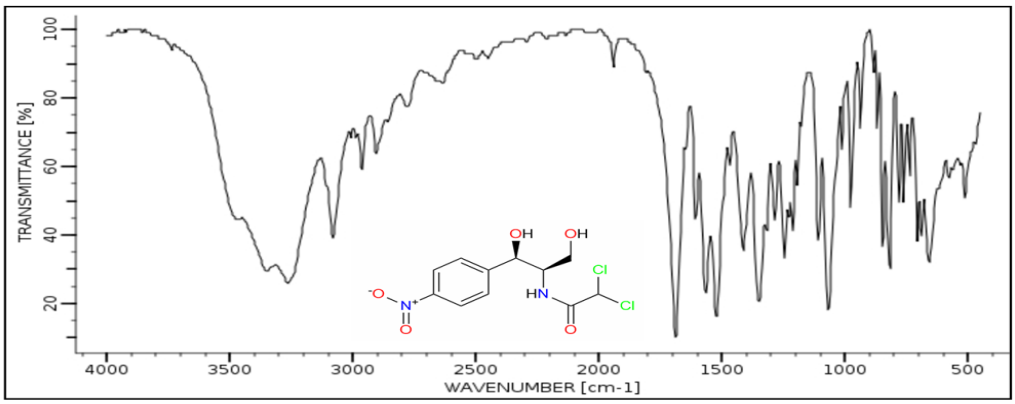

Figure 05: IR spectrum of Chloramphenicol.

Table 04: Infrared Absorption Band Assignment for Chloramphenicol.

Wavenumber (cm^{-1})	Assignment
O-H St.	3580
N-H St.	3468,3349
C-H Aromatic St.	3010
CH_2 Asym. St.	2923
CH_2 Sym. St.	2854
C=O St.	1686
N-H St.	1603
Ring St.	1574,1565
CNH	1550
C-C	1534
CH	1461378
C-NO_2	1348
C-N	1244
CO-H	1164,1060
C-O St.	1091
Ring Breathing	996
Ring Deformation	934,843
Skeletal St.	889
C-Cl	702,686,655

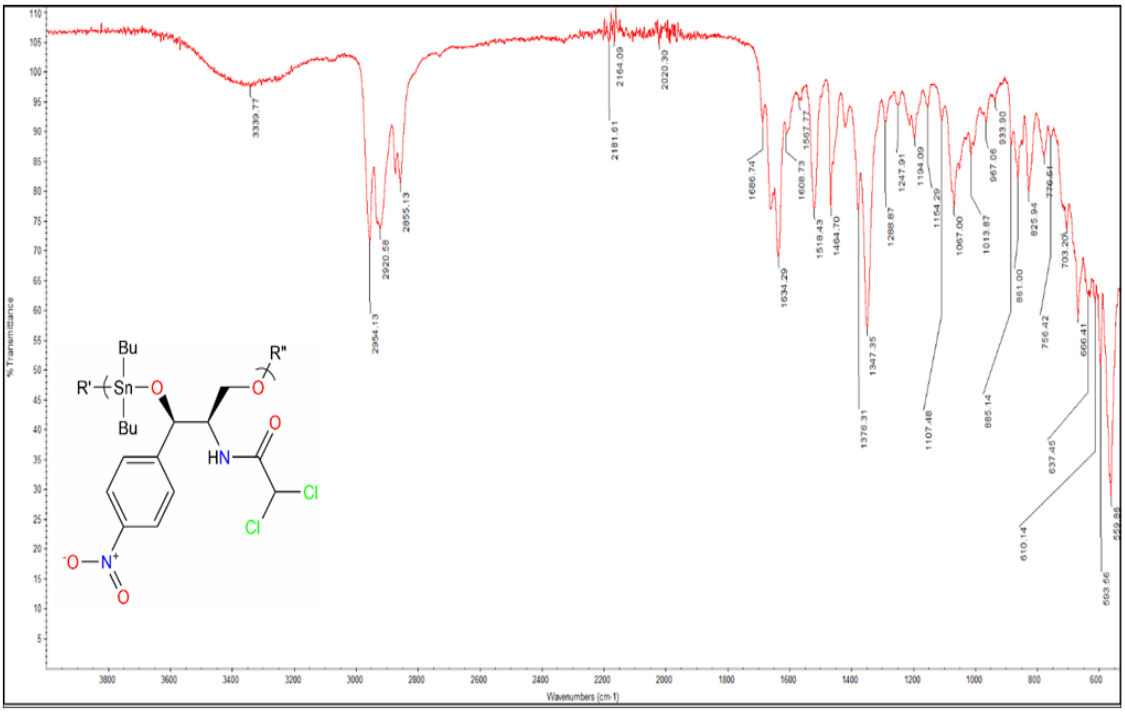

Figure 06: IR spectrum of Bu_2Sn_2Cl Polymer.

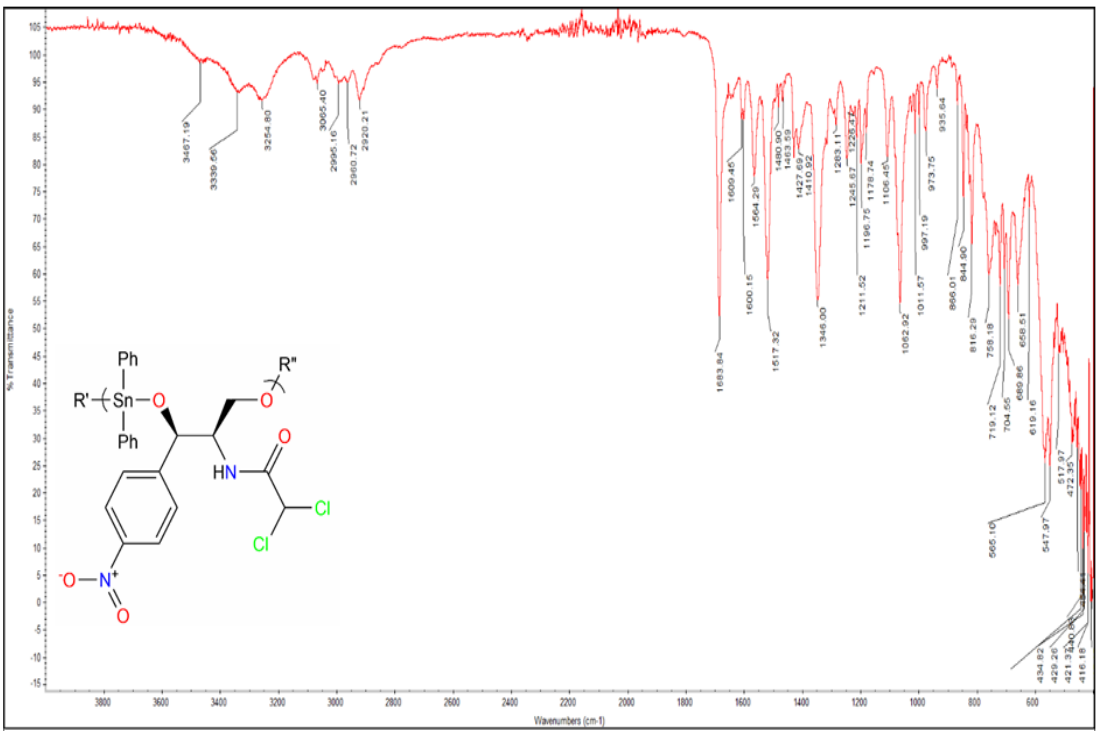

Figure 07: IR spectrum of Ph_2Sn_2Cl Polymer.

Table 05: Assigned Peaks for the monomers and associated polymers derived from reaction with chloramphenicol and dibutyl tin dichloride and diphenyl tin dichloride. (St.=Stretch).

Band Assignment	Chloramphenicol	Bu_2SnCl_2	Bu_2Sn/ Polymer	Ph_2SnCl_2	Ph_2Sn/ Polymer
O-H St.	3580	-	-	-	-
N-H St.	3468,3349	-	3340	-	3340
C-H Aromatic St.	3010	-	3012	3068,3051	3080,3065,
CH_3 Asym. St.	-	2959	2958	-	-
CH_2 Asym. St.	2923	2926	2921,2935	-	2920
CH_3 Sym. St.	-	2872	2874	-	-
CH_2 Sym. St.	2854	2858	2854,2855	-	2865
C=O St.	1686	-	1687	-	1684
N-H St.	1603	-	-	-	-
Ring St.	1574,1565	-	1587,1572	-	1567
CNH	1550	-	1540	-	1517
C-C	1534	-	1567	-	1564
Sn-Ph St.	-	-	-	1480	1481
C=C St.	-	-	-	1432	1428
CH	1461378	-	1465,1376	-	1464,1346
C-NO_2	1348	-	1347	-	1346
C-N	1244	-	1248	-	1246
CO-H	1164,1060	-	-	-	-
C-C St.	-	1178,1152	1194,1154	-	-
C-O St.	1091	-	1097	-	1106
Sn-O Asym. St.	-	-	1067	-	1063
Sn-Ph St.	-	-	-	1071	1070
Ring Breathing	996	-	986	996	997
Ring Deformation	934,843	-	934,845	-	936,845
Skeletal St.	889	-	892	-	890
CH_3 Rock	-	878	873	-	-
Sn-O Sym. St.	-	-	777	-	768
Sym. Op. Bend H's	-	-	-	729	735
C-Cl	702,686,655	-	703,667,642	-	705,690,659
Asym. Op Bend Ring	-	-	-	691	690
Sn-CH_2 Asym. St.	-	592	594	-	-
Sn-CH_2 Sym. St.	-	509	511	-	-
Sn-Ph Asym. St.	-	-	-	442	441
Sn-O Bend	-	-	419	-	416

Comparison of IR Spectral Band Assignments for Polymers and Monomers: All spectra showed bands characteristic of both reactants and new bands for the products, which were assigned to be the Sn-O linkage. A Sn-O symmetric stretch, asymmetric stretch, and a bend associate bands were found assigned to all the polymer products. For instance, in the region of about 3000 cm^{-1}, bands are found to contain the presence of the organotin and

chloramphenicol units in the product. The existence of the nitrate in chloramphenicol's structure is shown by bands consistent with the C-NO_2 moiety. Furthermore, the absence of bands associated with the OH functional group in the product is found as is expected. Also, bands associated with the amine moiety are moved consistent with it now being a NH unit rather than NH_2. Therefore, all bands assigned are consistent with polymer formation from the reaction between chloramphenicol and organotin dichlorides.

Matrix Assisted Laser Desorption Ionization Mass Spectrometry Results: To obtain good MALDI samples, the polymer and matrix need to readily form mixed polymer/matrix mixtures, which provide direct contact between the matrix and polymer sample. Because of this requirement, the polymer and matrix must both be soluble in a suitable volatile solvent such as water and acetone. However, the polymers described here are only soluble in a non-volatile liquid, DMSO, and thus this technique cannot be employed. To circumvent these solubility problems, a new analytical protocol for MALDI analysis has been found, involving a solid/solid sample preparation for polymers that are insoluble in MALDI-compatible solvents.[4-6,8,10-12,15,16] During the ionization event, high fragmentation of the polymeric materials occurs. The laser provides enough energy to break the bonds adjacent to a heteroatom and/or tin (Figure 8).

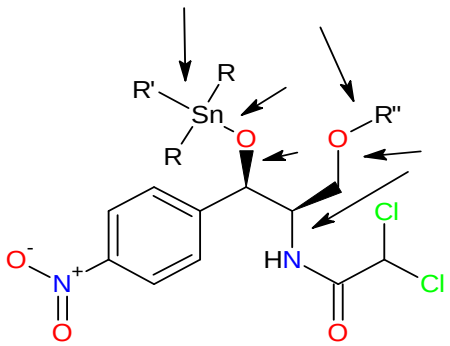

Figure 08: Major sites of bond scission of organotin polymers from chloramphenicol.

As a result, the peaks observed in the spectra occur from shorter fragments created when the laser hits the polymer, and not from the entire polymer. Furthermore, when different ion fragments are created that have the same structural formula, their mass-to-charge ratio differs based on the tin isotope present; this is because tin has ten different isotopes of which seven are present in amounts greater than 5%. Spectral fingerprints are created characteristic of the natural abundance of these isotopes. The structure of these fragments is determined by comparing fragment clusters to the calculated fingerprints of ion clusters. In the

determination of the number of tin atoms present in an ion fragment cluster, the isotopic abundance is significant. After the number of tin molecules in a fragment is known, the rest of the fragment can be elucidated by adding up the molecular weight of the components of the repeating units. This is done until the molecular weight of the elucidated fragments agrees with the peak fragment on the spectrum. To describe the assignments of the ion fragment structure, abbreviations are utilized. The following are the abbreviations used: Sn for the organotin moiety, C for the intact chloramphenicol unit minus two protons, O for oxygen, A for amide moiety, U for one repeat unit, 2U for two repeat units, etc. Note that sodium is common contaminant. Figures 9 and 10 contain the MALDI MS spectra for the dimethyltin dichloride and dioctyltin dichloride products from chloramphenicol over the approximated mass range of 500-1000 daltons, respectively. Tables 6-9 and show the identification of the fragments and their isotopic abundance matches for the previously mentioned products.

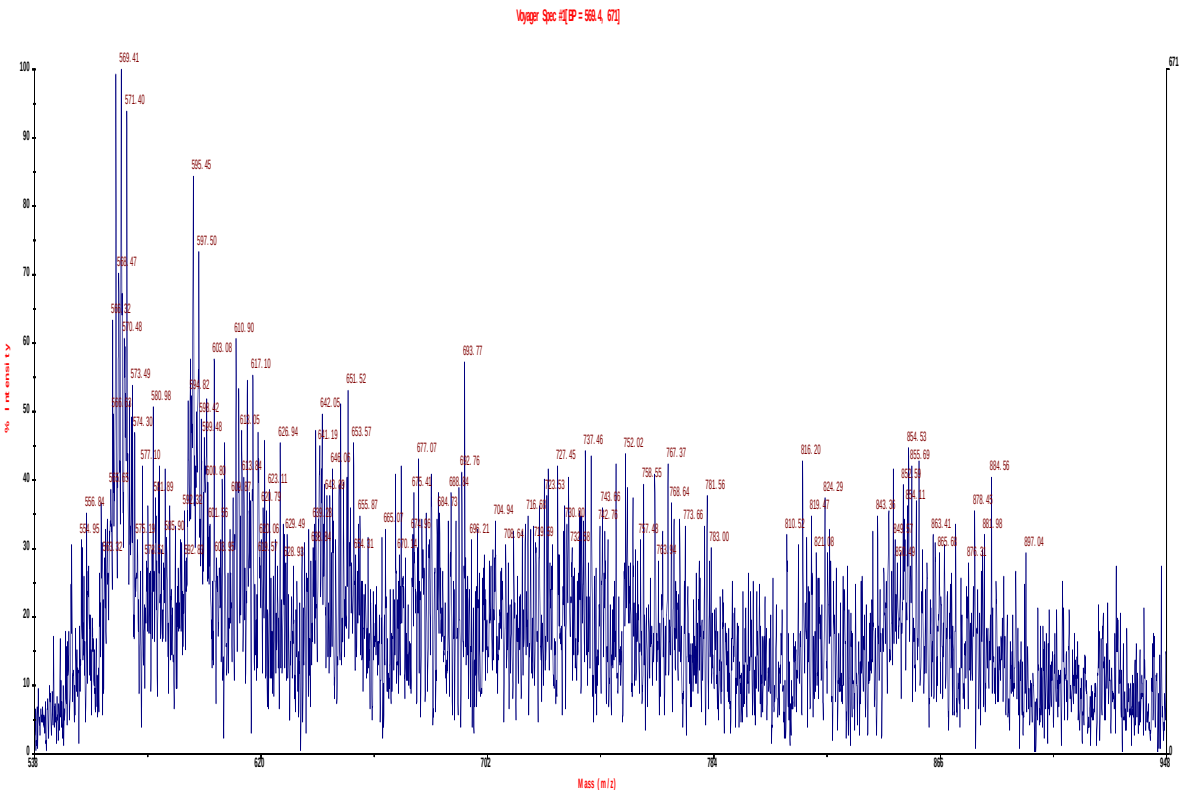

Figure 9: MALDI MS for the product of dimethyltin dichloride and chloramphenicol over the approximate mass range of 500 to 1000 Da.

Table 06: Major ion fragments and identification of the fragments for the product of dimethyltin dichloride and chloramphenicol over the approximate mass range of 500-1000 daltons (Da).

Mass (Da)	(Tentative) Structural Assignment
569	U+C, O-2A
652	U+Sn, 2O
694	2U-2A
855	2U+O, Na-A
879	2U+C-2A
970	2U+Sn-A
1016	2U+C-2A
1047	2U+C, O, Na-2A
1139	2U+C-A
1187	3U+Sn-3A
1217	3U+Sn, O, Na-3A
1314	3U+Sn-2A
1399	4U+C, O, Na-3A
1491	3U+C-2A
1528	4U+Na-4A
1639	4U-2A
1701	3U+C-2O
1757	4U-A
1793	4U+Sn-2A
1894	4U+Sn, O-A
1947	4U+Sn, O, Na-A
2195	4U+C-O
2294	5U+Sn, O, Na-2A

Ion fragment clusters to 5 units are found, which is consistent with the products being polymeric. Furthermore, these regions can be further studied by comparing the observed relative ion intensities found in the MALDI MS spectrum of the sample to the relative abundance observed in nature for tin isotopes. Table 7 contains such matches for ion fragments containing one and two tin atoms for the product of dimethyltin dichloride and chloramphenicol.

Table 7: Isotopic abundance matches for two tin-containing ion fragment clusters containing two tin atoms derived from the product of dmethyltin dichloride and chloramphenicol (Only ion fragments with >5% relative abundance are reported).

Known for Sn		2U+Sn, 2O		2U+O, Na+(-A)	
Mass (Da)	% Rel. Abu.	Mass (Da)	% Rel. Abu.	Mass (Da)	% Rel. Abu.
232	12	646	11	849	13
233	13	647	13	850	15
234	43	648	44	851	45
235	35	649	35	852	34
236	94	650	93	853	90
237	51	651	52	854	52
238	100	652	100	855	100
239	35	653	35	856	32
240	81	654	82	857	82
242	32	656	32	859	30
244	22	658	21	861	24

The agreement with the known relative abundances is consistent with the presence of tin atoms in the ion fragment clusters. At higher masses, isotope matches are difficult because of the low intensities of these generated ion fragments.

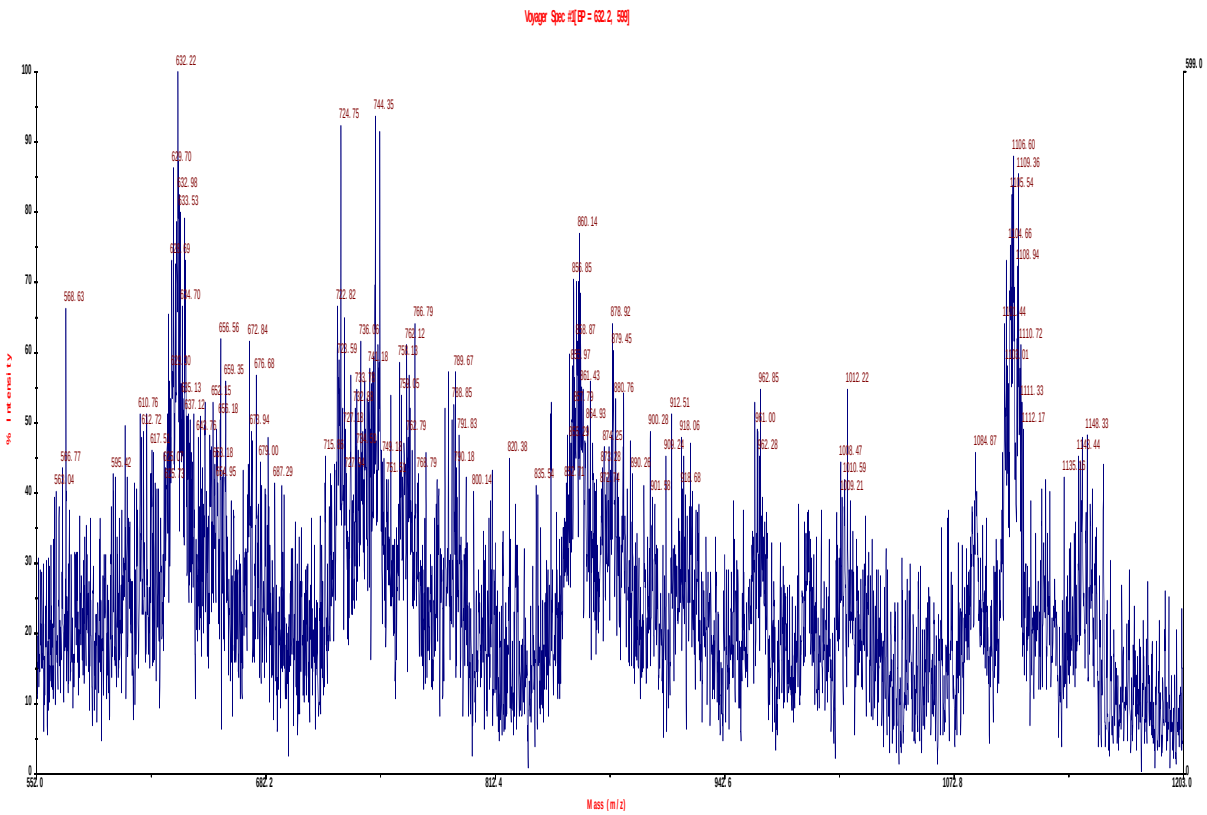

Figure 10: MALDI MS for the product of dioctyltin dichloride and chloramphenicol over the approximate mass range of 550 to 1200 Da.

Table 08: Major ion fragments and identification of the fragments for the product of dioctyltin dichloride and chloramphenicol over the approximate mass range of 500-1000 daltons (Da).

Mass (Da)	(Tentative) Structural Assignment
569	U+O-Oc
632	U+C-2A, Oc
744	U+C-A, Oc
860	U+C-A
879	U+C-Oc
963	2U-2A, Oc
1012	U-Sn
1107	2U+O-A, Oc
1143	2U+C-3A, Oc, O
1241	2U-Oc
1327	2U
1469	2U+Sn, O, Na
1544	2U+C
1558	2U+Sn-A
1606	3U-3A, O
1663	2U+C
1691	2U+Sn, O
1731	3U-A, Oc, Na
1779	3U+O-A, Oc
1824	3U-4A, Oc
1858	3U+Sn-3A, Oc
1901	3U+Na-A
1954	3U+C-2A, Oc
1980	3U-2A, Oc
2041	4U-4A, Oc
2074	4U+Na-4A, Oc
2133	3U+Sn, Na-A, Oc
2160	4U, Na-3A, Oc
2184	4U+O-3A, Oc
2231	3U+Sn-Oc
2267	3U+Sn, O
2294	4U-3A
2337	4U+C-5A
2370	4U+C-4A, Oc
2382	4U+C, O-5A
2422	4U-2A
2442	4U+Na-2A

Ion fragment clusters to 4 units are found. Tables 11 and 12 contain the isotopic abundance matches for one and two tin atoms. The matches are in agreement with the known percentage isotopes and consistent with the ion fragment clusters containing one and two tin atoms within the clusters.

Table 09: Isotopic abundance matches for ion fragment clusters containing one tin atom derived from the product of dioctyltin dichloride and chloramphenicol (Only ion fragments with >5% relative abundance are reported).

Known for Sn		U+O+(-Oc)		U+C+(-2A), Oc	
Mass (Da)	% Rel. Abu.	Mass (Da)	% Rel. Abu.	Mass (Da)	% Rel. Abu.
116	45	565	47	628	46
117	24	566	23	629	22
118	75	567	71	630	78
119	26	568	25	631	26
120	100	569	100	632	100
122	14	571	15	634	14
124	17	572	18	636	18

Table 10: Isotopic abundance matches for ion fragment clusters containing two tin atoms derived from the product of dioctyltin dichloride and chloramphenicol (Only ion fragments with >5% relative abundance are reported).

Known for Sn		2U+Sn, 2O		2U+O, Na+(-A)	
Mass (Da)	% Rel. Abu.	Mass (Da)	% Rel. Abu.	Mass (Da)	% Rel. Abu.
232	12	957	12	1006	11
233	13	958	12	1007	12
234	43	959	42	1008	44
235	35	960	36	1009	35
236	94	961	93	1010	88
237	51	962	53	1011	47
238	100	963	100	1012	100
239	35	964	32	1013	32
240	81	965	76	1014	72
242	32	967	31	1016	30
244	22	969	23	1018	24

The agreement with the known relative abundances is consistent with the presence of tin atoms in the ion fragment clusters. Overall, the MALDI MS spectra showed ion fragments with 3-5 units with good isotopic abundance matches to the presence of tin in the ion fragments.

Cancer Cell Lines: As noted before, a major purpose in synthesizing metal-containing polymers is to investigate their ability to inhibit unwanted pathogens and infectious agents. Here the focus is cancer. Table 11 contains the cell lines employed in the current study. These are all human cell lines.

Table 11: Cell lines employed in the current study.

Strain Number	NCI Designation	Species	Tumor Origin	Histological Type
3465	PC-3	Human	Prostate	Carcinoma
7233	MDA MB-231	Human	Pleural effusion breast	Adenocarcinoma
1507	HT-29	Human	Recto-sigmoid colon	Adenocarcinoma
7259	MCF-7	Human	Pleural effusion-breast	Adenocarcinoma
ATCC CCL-75	WI-38	Human	Normal embryonic lung	Fibroblast
	U251	Human	Glioblastoma multiforme	Astrocytomas
	G55	Human	Glioblastoma	Astrocytomas
	AsPC-1	Human	Pancreatic cells	Adenocarcinoma
	PANC-1	Human	Epithelioid pancreatic cells	Carcinoma

The two most widely used approaches employed to evaluate cell line data are used in the present study. The first approach measures the concentration dose needed to reduce the growth of the particular cell line. The term effective concentration, EC, is used here to describe this measure. The amount of a tested material that induces inhibition halfway between the baseline and maximum is referred to as the 50% response concentration and given the symbol EC_{50}. EC_{50} values for the monomers and polymers, including values for cisplatin as a standard, are given in Table 9. Cisplatin is a widely used anticancer drug. It is toxic as indicated by the low EC_{50} values for the standard cell line WI-38. In combating cancer cisplatin, and other related platinum drugs, exhibit many unwanted side effects in patients including loss of hair, loss of taste, numbness, vomiting, kidney damage, hearing loss, etc.[25] Even so, it remains among the most widely employed drugs for the treatment of cancer but because of the unwanted side-effects, alternatives are sought.[25]

For the current study several observations are found. All of the monomers and polymers inhibit all of the cancer cell lines. This is not typical since in most other studies, the non-tin containing drug does not inhibit the cancer cells. Even so, for a majority of the cases, the polymers are more toxic towards the cancer cell lines compared with chloramphenicol. Second, in general the polymers exhibit better inhibition of the cancer cell lines compared with the organotin monomers. Exceptions occurs. Thus, towards the pancreatic cancer lines, the dibutyltin dichloride itself exhibits high toxicity towards the cancer cell lines compared with the polymer.

The following focuses on the ability of the polymers to inhibit specific cancer cell lines. There is no effective treatment of pancreatic cancer once it metastasizes. In the USA yearly about 32,000 new cases are diagnosed yearly. Within a year almost all patients die.

Worldwide, it is the fourth leading cause of cancer death. We found that inhibition of pancreatic cancer cell lines is difficult compared with other human cancer cell lines (excepting brain cancer). Even so, we found a number of organotin polymers that exhibit good ability to inhibit pancreatic cancer. In the current study the two most widely studied human pancreatic cancer cell lines are used. The tested cell lines are AsPC-1 which is an adenocarcinoma pancreatic cell line, which accounts for about 80% of the diagnosed human pancreatic cancers, and PANC-1 which is an epithelioid carcinoma pancreatic cell line, accounting for about 10% of the human pancreatic cancer cases. In the current study, the organotin polymers show decent inhibition of both cell lines with the inhibition similar for the two cell lines. This similarity is consistent with the idea that the polymers may offer broad-spectra inhibition of other pancreatic cancer cell lines.

Recently we begun to look at the ability of our polymers to inhibit the growth of human glioblastoma brain cancer. Like pancreatic cancer, the expected life expectancy once glioblastoma cancer is found is less than a year. G55 is a relatively new human glioblastoma cell line. It was developed by C. David James (Department of Neurological, University of California San Francisco. It is a human glioblastoma cell line that had been passed through nude mice and re-established as a stable xenograft cell line. The U251 cell line is one of the most used cancer cell lines. It is derived from a human malignant glioblastoma multiforme. Astrocytomas are brain cancer that originates in astocytes. High-grade astocytomas, called glioblastoma multiforme, are the most malignant of all brain tumors. Studies involving various cancer cell lines show that the G55 cells tend to be more invasive more accurately modeling brain cancer because of this greater invasiveness and migration since they form invasive intracranial tumors in rodents more characteristic of primary human glioblastoma multiforme, GBM. There is no decent chemo treatment for brain cancer thus the ability to inhibit it by treatment with chemo drugs is greatly needed. The current organotin polymers show ability to inhibit both types of brain cancer cell lines (Table 9). The inhibition is better, generally lower EC_{50}, for the polymers compared with the organotin monomers and chloramphenicol.

Table 12: EC_{50} values, micrograms/mL, for the monomers and polymers.

Sample	*WI-38*	*PANC-1*	*AsPC-1*	*PC-3*
Me_2SnCl_2	0.22(.1)	0.80(.1)	0.71(.1)	0.51(.1)
Me_2Sn/CH	0.36(.02)	0.21(0.04)	0.27(0.04)	0.26(.01)
Et_2SnCl_2	0.20(.1)	0.48(.1)	0.90(.1)	0.61(.1)
Et_2Sn/CH	0.31(.07)	0.35(.08)	0.37(.03)	0.24(.06)
Bu_2SnCl_2	0.20(.05)	0.0032(.001)	0.012(.01)	1.4(1.1)
Bu_2Sn/CH	0.21(.03)	0.26(.07)	0.37(.06)	0.25(.03)
Oc_2SnCl_2	0.30(.1)	0.85(.1)	0.85(.1)	0.55(.1)
Oc_2Sn/CH	0.31(.04)	0.28(.05)	0.37(.01)	0.38(.06)
Ph_2SnCl_2	0.25(.1)	0.71(.1)	0.83(.1)	0.82(.1)
Ph_2Sn/CH	0.39(.03)	0.38(.01)	0.39(.01)	0.20(.09)
Chloramph	0.22(.06)	0.31(0.06)	0.28(0.01)	0.35(.05)
Cisplatin	0.012(.01)	0.0023(.005)	0.0035(.005)	0.0044(.004)

Sample	*MDA-MB-231*	*HT-29*	*MCF-7*	*U251*	*G55*
Me_2SnCl_2	0.44(.1)	0.56(.1)	0.66(.1)	0.91(0.5	1.2(0.6)
Me_2Sn/CH	0.29(.06)	0.34(.08)	0.27(.05)	0.24((.03)	0.26(.03)
Et_2SnCl_2	0.64(.1)	0.71(.1)	0.77(.1)	1.1(0.6)	0.76(0.7)
Et_2Sn/CH	0.37(.06)	0.31(.04)	0.24(.02)	0.34(0.9)	0.29(.02)
Bu_2SnCl_2	1.4(1.3)	1.2(.1)	0.70(.06)	1.0(0.2)	1.0(0.4)
Bu_2Sn/CH	0.26(.02)	0.34(.09)	0.38(.05)	0.24(.08)	0.21(.05)
Oc_2SnCl_2	0.65(.1)	0.65(.1)	0.70(.1)	1.3(0.7)	0.95(0.6)
Oc_2Sn/CH	0.37(.08)	0.34(.01)	0.30(.07)	0.32(.02)	0.30(.07)
Ph_2SnCl_2	0.76(.1)	0.56(.1)	0.68(.1)	0.89(0.6)	0.97(0.6)
Ph_2Sn/CH	0.31.(0.01)	0.21(.09)	0.24(.04)	0.34(.08)	0.37(.04)
Chloramph	0.36(0.01)	0.26(.05)	0.37(.01)	0.35(.02)	0.28(.08)
Cisplatin	0.0029(.002)	0.0041(.003)	0.0057(.003)	0.015(0.01)	0.021(0.01)

The second calculation for measuring anticancer effectiveness is called the chemotherapeutic index, CI, where the CI_{50} is the ratio of the EC_{50} for the standard cell line WI-38 cells divided by the EC_{50} for the test cell. These results are shown in Table 10. Values greater than one are desirable in this measure since it indicates that there is a preference for inhibiting the cancer cell lines in comparison to the standard cells. In the present case, there are a number of CI values greater than one and the values for the polymers are typically greater than those for the monomers consistent with the idea that combining the organotin moiety with the chloramphenicol shows a positive behavior in the ability to inhibit the cancer cell lines.

Table 13: CI values for the polymers and monomers based on values given in Table 12.

Sample	EC_{50}WI-38/ EC_{50}PNC-1	EC_{50}WI-38/ EC_{50}AsPC-1	EC_{50}WI-38/ EC_{50}PC-3	EC_{50}WI-38/ EC_{50}MDA
Me_2SnCl_2	0.28	0.31	0.43	0.50
Me_2Sn/CH	1.7	1.3	1.4	1.2
Et_2SnCl_2	0.83	0.81	0.91	0.91
Et_2Sn/DG	0.89	0.84	1.3	1.1
Bu_2SnCl_2	60	17	0.14	0.14
Bu_2Sn/CH	0.81	0.57	0.81	O.81
Oc_2SnCl_2	0.35	0.35	0.55	0.46
Oc_2Sn/CH	0.81	0.79	1.6	0.84
Ph_2SnCl_2	0.35	0.31	0.30	0.33
Ph_2Sn/CH	1.0	1.0	2.0	1.2
Cisplatin	5.2	3.4	2.7	4.1

Sample	EC_{50}WI-38/ EC_{50}HT-29	EC_{50}WI-38/ EC_{50}MCF-7	EC_{50}WI-38/ EC_{50}U251	EC_{50}WI-38/ EC_{50}G55
Me_2SnCl_2	0.39	0.39	0.45	0.31
Me_2Sn/CH	1.1	0.97	1.5	1.4
Et_2SnCl_2	0.67	0.71	0.34	0.29
Et_2Sn/DCH	1.0	1.3	0.81	1.2
Bu_2SnCl_2	0.17	O,29	0.33	0.33
Bu_2Sn/CH	0.62	0.55	0.88	0.10
Oc_2SnCl_2	0.46	0.43	0.34	0.46
Oc_2Sn/CH	0.91	1.0	O.97	1.0
Ph_2SnCl_2	0.45	0.37	0.29	0.30
Ph_2Sn/CH	1.5	1.3	0.91	0.84
Cisplatin	2.9	2.1	0.80	0.57

Table 11 contains the CI_{50} values based on the WI-38 standard human cell line.

Thus, the current polymers show decent inhibition of the cancer cell lines based on EC_{50} and CI values.

CONCLUSIONS

Organotin polyesters are rapidly formed in moderate yields from the interfacial polymerization of organotin dihalides with chloramphenicol. Yield and chain length decrease as the organotin alkyl chain length increase. IR spectroscopy shows bands consistent with the formation of Sn-O ether linkages. MALDI MS shows formation of ion fragments containing tin to four and five units long. The polymers exhibit good inhibition of all of the tested cancer cell lines including pancreatic, breast, and brain cancer cell lines. Because of the breath of cancer cell line inhibition, they offer an additional family of potential anticancer materials.

REFERENCES

1. Hadjikakou SK, Abdellah MA, Hadjiliadis N, Kubicki M, Bakas T, Kourkoumelis N, Simos YV, Karkabounas S, Barsan MM, Butler IS. Synthesis, Characterization, and Biological Studies of Organotin(IV) Derivatives with o- or p-Hydroxybenzoic Acids. Bioinorg Chem Appl, 2009; 2009: 542979.
2. Piver WT. Organotin Compounds: Industrial Applications and Biological Investigation. Environmental Health Perspectives, 1973; 4: 61-79.
3. Carraher CE. Organotin Polymers. 2005; 263-310.
4. Carraher CE, Roner MR, Campbell A, Moric-Johnson A, Miller L, Slawek P, Mosca F, Einkauf J, Haky J, Crichton R. Synthesis of Organotin Polyesters from Reaction of the Salt of D-Camphoric Acid and Organotin Dihalides and Initial Anticancer Activity. J Inorg Organomet Polym Mat, 2018; 28: 481-491.
5. Carraher CE, Roner MR, Patel D, Milller L, Moric-Johnson A, Slawek P, Mosca F, Frank J. Synthesis of organotin polymers from 2-ketoglutaric acid and their ability to inhibit the growth of human cancer cell lines. Hematology Medical Oncology, 2018; 3(1): 1-9.
6. Carraher CE, Roner MR, Islam Z, Moric-Johnson A. Group 15 organotin containing polyamines from histamine and their ability to inhibit cancer cell lines from pancreatic, breast and other cancers. J Pharmacy & Pharmacetical Res., 2018; 2(1): 1-10.
7. Carraher CE, Roner MR, Slawek P, Mosca F. Group 4 metallocene polymers-selected properties and applications. Inorganics, 2018; 6(65): 1-14.
8. Carraher CE, Roner MR, Lynch M, Moric-Johnson A, Miller L, Slawek P, Mosca F, Frank J. Organotin poly(ester ethers) from salicylic acid and their ability to inhibit human cancer cell lines. Journal of Clinical Research in Onology, 2018; 1: 1-11.
9. Carraher CE**,** Roner MR, Shahi K, Moric-Johnson A, Miller L, Slawek P, Mosca F. Control of breast cancer using metal-containing polymers based on cell line results. Annals of Breast Cancer, 2018; 1(1003): 1-9.
10. Carraher CE, Roner MR, Slawek P, Mosca F, Frank J, Miller L. Groups 4 and 15 and organotin condensation polymes for the treatment of cancers and viruses. MAMS, 2018; 1: 9-14.
11. Carraher CE, Roner MR, Frank J, Mosca F, Slawek P, Miller L. Inhibition of human glioblastomas brain cancer cell lines by metal-containing polymers. WJPR, 2019; 8(6): 123-139.
12. Carraher CE, Roner MR, Frank J, Black K, Moric-Johnson A, Miller L, Mosca F, Slawek P. Synthesis and initial anticancer activity of water and dimethyl sulfoxide soluble polyethers from zirconocene dichloride and poly(ethylene glycols). WJPR, 2019; 8(7): 63-84.

13. Carraher CE, Roner MR, Frank J, Slawek P, Mosca F, Shahi K, Moric-Johnson A, Miller L. Organotin polymers for the control of pancreatic cancer. OBM Hepatology & Gastroenterology, 2019; 3(2): 1-10.
14. Carraher CE, Roner MR, Crichton R, Frank J, Moric-Johnson A, Miller LC, Mosca F, Slawek P. Synthesis and cancer inhibition of polyamines from reaction of 3-amino-1,2,4-triazole (3-AT) and group 4 metallocene dihalides. European Journal Pharmaceutical and Medical Research, 2019; 6(8): 153-163.
15. Carraher CR, Roner MR, Crichton R, Frank J, Moric-Johnson A, Miller LC, Mosca F, Slawek P. Polyamines from reaction of organotin dihalides and 3-amino-1,2,4-triazole (3-AT)-synthesis and ability to inhibit human cancer cell lines. WJPR, 2019; 8(10): 39-58.
16. Carraher CE, Mosca F, Roner MR, Slawek P, Moric-Johnson A, Miller L, Haky JE. Synthesis of organotin poly(amine ethers) from the HIVG drug lamivudine (3TC). European Journal Pharmaceutical and Medical Research, 2019; 6(9): 42-58.
17. Carraher CE, Slawek P, Roner MR, Mosca F, Moric-Johnson A, Miller L, Haky J. Amino acid organotin polymers from diglycine-synthesis, structural characterization and initial anticancer activity. J Inorg Organomet Polym Mat, 2020; 30: 182-195.
18. Roner MR, Carraher CE, Miller L, Mosca F, Slawek P, Haky J, Frank J. Organotin polymers as antivirial agents including inhibition of zika and vaccinia viruses. J Inorg Organomet Polym Mat, 2020; 30: 684-694.
19. Abd-El-Aziz AS, Carraher CE, Pittman CU, Zeldin M. Macromolecules Containing Metal and Metal-Like Elements: Group IVA Polymers, 2005.
20. Schifano JM, Edifor R, Sharp J D, Ouyang M, Konkimalla A, Husson RN, Woychik NA. Mycobacterial Toxin MazF-Mt6 Inhibits Translation through Cleavage of 23S RRNA at the Ribosomal A Site. Proc Natl Acad Sci., 2013; 110(21): 8501-8506.
21. Molesworth AM, Cuevas LE, Connor SJ, Morse AP, Thomson MC. Environmental Risk and Meningitis Epidemics in Africa. Emerg Infect Dis., 2003; 9(10): 1287-1293.
22. Carraher CE. Polymer Chemistry, NY: Taylor and Francis, 2018.
23. Carraher CE. Introduction to Polymer Chemistry, Taylor and Francis, 2017.
24. El-Wahed MGA, Refat MS, El-Megharbel SM. Spectroscopic Studies on the Complexation of Some Transition Metals with Chloramphenicol Drug. J Mol Struct, 2008; 1: 402-413.
25. Oun R, Moussa YE, Wheate NJ. The side effects of platinum-based chemotherapy drugs: a review for chemists. Dalton Trans, 2018; 47: 6645-6653.